Dosimetry of the I-Plant Model 3500 iodine-125 brachytherapy source

D. M. Duggan and B. L. Johnson
Department of Radiation Oncology, Vanderbilt University Medical Center, Nashville, Tennessee 37232-5671

(Received 14 September 2000; accepted for publication 31 January 2001)

^{125}I brachytherapy sources have been widely used for interstitial implants for a number of years in several tumor sites, especially the prostate. The design of the new I-Plant Model 3500 iodine source is novel, yet its characteristics are similar to those of two existing designs, Model 6711 and the Symmetra. Dosimetry parameters (including dose rate constant, radial dose function, and anisotropy function, as defined by AAPM Task Group 43) were measured with LiF thermoluminescent dosimeters in water-equivalent plastic phantoms. The dose rate constant was found by direct comparison of calibrated I-Plant Model 3500 and Model 6711 seeds in a solid water phantom, to be 1.01 (cGy/h)/U. The radial dose function and anisotropy function are similar to those of the Model 6711 and Symmetra seeds. © *2001 American Association of Physicists in Medicine.*
[DOI: 10.1118/1.1357456]

Key words: dosimetry, ^{125}I, Task Group 43, brachytherapy

I. INTRODUCTION

The use of ^{125}I seed sources for interstitial implants in several tumor sites, including the eye,[1–5] brain,[6–9] and prostate, is well established.[10–14] Ultrasound-guided prostate implants have become especially popular in recent years as an alternative to radical prostatectomy because they are cost effective[15] and cause few side effects.[16] As a result, a number of new seed designs have been introduced in just the last few years.[17–22] A new design, the I-Plant Model 3500 source (Implant Sciences Corporation, Wakefield, MA), is similar to the Model 6711 (Medi-Physics, Inc., Arlington Heights, IL),[23–30] and the Symmetra (Bebig GmbH, Berlin, Germany) seeds but is made by a novel process that facilitates ''just-in-time'' manufacturing. Before it is used in patients the dosimetric parameters defined in the report of AAPM Task Group 43 (TG-43) must be obtained.[31,32] In the present study the complete set of parameters required for dose calculation using the TG-43 formalism was acquired using LiF thermoluminescent dosimeters (TLD) in water-equivalent plastic phantoms. Monte Carlo simulations, performed with the MCNP4B code, were used for converting dose measured in a water-equivalent phantom to dose in water.

II. MATERIALS AND METHODS

A. ^{125}I source

As shown in Fig. 1, the new seed design resembles that of the Model 6711 (Medi-Physics, Inc., Arlington Heights, IL) but with an important difference. The silver rod in the center is surrounded by a glass tube and the ^{125}I is on the outer surface of the glass. In the novel manufacturing process, ^{124}Xe is ion-implanted into the outer surface of the glass to make the inner core. This nonradioactive inner core can be stored until seeds are needed. Then it is activated and placed into the titanium capsule, which is then welded shut. The outer dimensions of the seed are compatible with all applicators. The diameter and length of the inner core are quite close to the inner diameter and length of the capsule to minimize movement of the core inside the capsule. The photon spectrum of the new seed was measured by NIST (National Institute of Standards and Technology, Gaithersburg, MD) and is presented in Table I.

B. TG-43 dose calculation formalism

According to the recommendations of AAPM Task Group 43,[31] the dose distribution in water surrounding an interstitial brachytherapy source should be calculated from

$$\dot{D}(r,\theta)=S_k\Lambda[G(r,\theta)/G(r_0,\theta_0)]g(r)F(r,\theta), \tag{1}$$

where S_k is the air kerma strength, Λ is the dose rate constant given by

$$\Lambda=\dot{D}(r_0,\theta_0)/S_k, \tag{2}$$

$r_0=1$ cm, $\theta_0=\pi/2$ (the plane through the seed center perpendicular to its axis), $G(r,\theta)$ is the geometry function discussed below, $g(r)$ is the radial dose function

$$g(r)=\frac{[\dot{D}(r,\theta_0)/\dot{D}(r_0,\theta_0)]}{[G(r,\theta_0)/G(r_0,\theta_0)]}, \tag{3}$$

and $F(r,\theta)$ is the anisotropy function

$$F(r,\theta)=\frac{[\dot{D}(r,\theta)/\dot{D}(r,\theta_0)]}{[G(r,\theta)/G(r,\theta_0)]}. \tag{4}$$

The geometry function $G(r,\theta)$ is calculated rather than measured. It accounts for the effects of the distribution of activity inside the source but not absorption or scattering and it is given by

$$G(r,\theta)=\frac{\int(\rho(\mathbf{r}')/|\mathbf{r}'-\mathbf{r}|^2)dV'}{\int\rho(\mathbf{r}')dV'}, \tag{5}$$

where $\rho(r')$ is the activity per unit volume at point r'. For simplicity, $G(r,\theta)$ was calculated for a line source so that

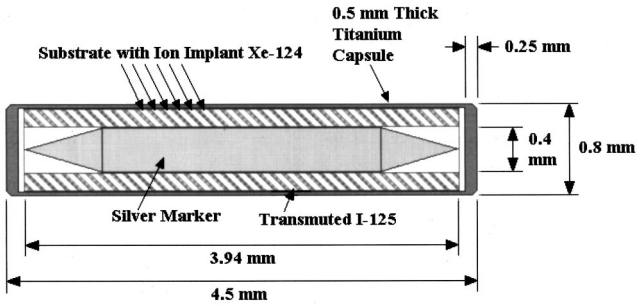

FIG. 1. Schematic drawing of the I-Plant Model 3500 brachytherapy source. The ^{125}I is embedded in a thin outer layer of the glass tube which surrounds the silver marker rod. It is made by a novel process in which ^{124}Xe is ion-implanted into the glass tube, which is then activated to become ^{125}I. Then the silver marker and glass tube are placed in the titanium capsule, which is sealed by welding.

$$G(r,\theta)=\frac{\tan^{-1}\left(\frac{x+L/2}{y}\right)-\tan^{-1}\left(\frac{x-L/2}{y}\right)}{Ly}, \qquad (6)$$

where L is the active length of the line source. The actual length of the glass tube, on the outer surace of which is the I-125, is 3.94 mm, but since there is a small tolerance on that dimension and the marker can move slightly, the active length was simply taken to be $L=4$ mm, the same as the inside length of the capsule. The calculated values of $G(r,\theta)$ are given in Table II.

C. Thermoluminescent dosimetry

The dose distribution around the I-Plant Model 3500 Iodine-125 source was measured with LiF TLD rods (Harshaw/Bicron, Solon, OH), all 1 mm in diameter and 3 mm long, placed in specially machined water-equivalent plastic phantoms. The phantom material for the dose rate constant measurement was solid water (Model 457, Radiation Measurements, Inc., Middleton, WI) but for all the other measurements, plastic water (Model PW 2030, Computerized Imaging Reference Systems, Inc., Norfolk, VA) was used. This plastic water was a special composition (Table III) designed to have scattering, and absorption coefficients nearly the same as those of water for photons with energies in the range 20 to 30 keV. As shown in Tables IV a and IV b, it is a close match to water for ^{125}I energies.

TABLE I. Measured photon spectrum of I-Plant Model 3500 seed.

Photon energy (keV)	Relative number
22.1	0.0058
24.9	0.0345
25.5	0.0107
27.2	0.2524
27.4	0.4641
31.0	0.1490
31.7	0.0342
35.5	0.0493

The dose rate constant phantom was the simplest in design, consisting of one central hole just big enough for a single seed surrounded by six holes for TLD rods, parallel to the seed, equally spaced around a 1 cm radius circle with the seed at its center. The phantom was made from solid water because correction factors for this material are available in the literature.[29,33]

The two plastic water phantoms used to determine the radial dose function are shown in Fig. 2. In the first phantom [Fig. 2(a)], the TLD rods are in close-fitting holes, equally spaced around circles, of radii from 0.5 to 7 cm at 0.5 cm intervals, with the seed at their center. There are three TLD holes at each distance, except at 1 cm, where there are six. The hole pattern was chosen to minimize interference between rods.[34] The second phantom [Fig. 2(b)] was used to obtain doses from 5 to 7 cm, where it is difficult to obtain high enough doses from a single seed for reliable measurements. In this phantom, four seeds were placed on a circle surrounding a TLD rod at the center. The phantom used to measure the anisotropy function is shown in Fig. 3. This also consists of holes for TLD rods arranged on circles with a seed at their center, in patterns designed to minimize interference between rods.[34] However, in this phantom the seed is perpendicular to the TLD rods. All the TLD rods at a given radius are in the same quadrant, taking advantage of the assumed symmetry of the dose distribution. The TLD rods were individually calibrated with a ^{60}Co beam, which in turn

TABLE II. Geometry function for a 4 mm line source calculated according to Eq. (6).

θ (deg) / r (cm)	0	10	20	30	40	50	60	70	80	90
0.5	4.7615	4.7192	4.6035	4.4442	4.2730	4.1140	3.9818	3.8843	3.8250	3.8051
1.0	1.0416	1.0399	1.0347	1.0270	1.0178	1.0083	0.9997	0.9929	0.9885	0.9870
1.5	0.4525	0.4522	0.4512	0.4497	0.4480	0.4461	0.4444	0.4430	0.4421	0.4418
2.0	0.2525	0.2524	0.2521	0.2517	0.2511	0.2505	0.2500	0.2496	0.2493	0.2492
2.5	0.1610	0.1610	0.1609	0.1607	0.1605	0.1602	0.1600	0.1598	0.1597	0.1597
3.0	0.1116	0.1116	0.1115	0.1114	0.1113	0.1112	0.1111	0.1110	0.1110	0.1109
3.5	0.0819	0.0819	0.0819	0.0818	0.0818	0.0817	0.0816	0.0816	0.0816	0.0815
4.0	0.0627	0.0627	0.0626	0.0626	0.0626	0.0625	0.0625	0.0625	0.0625	0.0624
5.0	0.0401	0.0401	0.0401	0.0400	0.0400	0.0400	0.0400	0.0400	0.0400	0.0400
6.0	0.0278	0.0278	0.0278	0.0278	0.0278	0.0278	0.0278	0.0278	0.0278	0.0278
7.0	0.0204	0.0204	0.0204	0.0204	0.0204	0.0204	0.0204	0.0204	0.0204	0.0204

TABLE III. Composition (by weight) of specially formulated plastic stin water PW2030 with density 1.022 g/cm^3.

Element	Weight percent
Carbon	61.25
Oxygen	19.89
Hydrogen	8.59
Nitrogen	1.56
Aluminum	8.44
Chlorine	0.21

had been calibrated in accordance with the AAPM Task Group 21 protocol.[35]

D. Monte Carlo simulation

The MCNP code, developed by Los Alamos National Laboratory,[36] has already been used successfully to model interstitial brachytherapy sources.[17,37] Its algorithms and cross-section libraries are thoroughly validated[38] and the user does not have to risk introducing errors by writing subroutines for finding distances to surfaces or computing tallies.

The correction factors for converting the radial dose function from plastic water to water were calculated by simulating point sources as recommended by Luxton.[29] Because the TLD rods are calibrated for dose-to-water, the correction factor is the ratio of the dose-to-water in plastic water (the dose to a small volume of water in an otherwise homogeneous, infinite plastic water medium) to the dose-to-water in water (in a homogeneous, infinite water phantom). All of the doses were calculated with a point source, with the spectrum shown in Table I, and spherical shell tally cells. In the case of the dose-to-water in plastic water the only tally cell is a

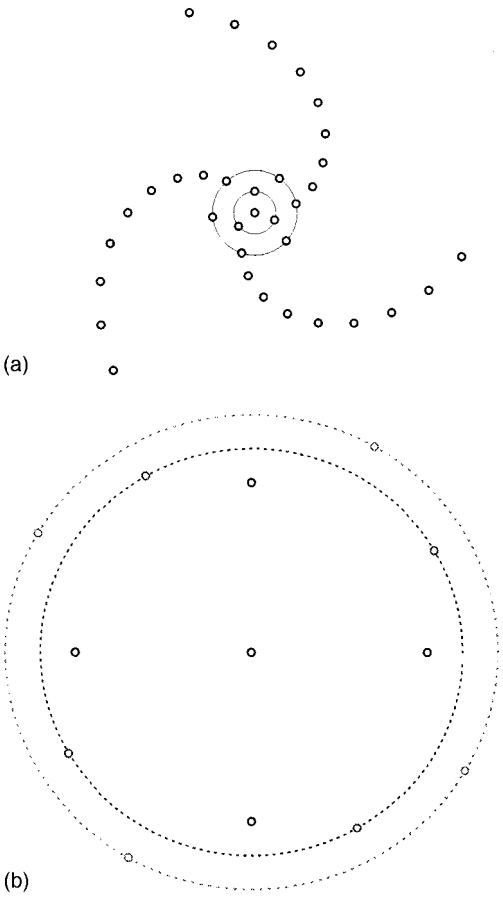

FIG. 2. Plastic water phantoms used for measuring the radial dependence of the dose rate from the I-Plant Model 3500 seed. (A) Seed in center surrounded by parallel LiF TLD rods, at least three at each radial distance (six 1 cm from seed). (B) Single TLD rod in center surrounded by four seeds, all at the same radial distance. Used to measure radial dose function for distances greater than 4 cm.

TABLE IV. (a) Scattering and absorption coefficients for water at I-125 energies. (b) Scattering and absorption coefficients for PW2030 at I-125 energies.

Photon energy (keV)	Coherent scattering coefficient (cm^2/g)	Incoherent scattering coefficient (cm^2/g)	Photoelectric absorption coefficient (cm^2/g)	Total attenuation coefficient (cm^2/g)	Energy absorption coefficient (cm^2/g)
			(a)		
22.1	7.63E−02	1.79E−01	3.94E−01	6.49E−01	4.020E−01
24.9	6.34E−02	1.81E−01	2.68E−01	5.12E−01	2.769E−01
25.5	6.11E−02	1.81E−01	2.48E−01	4.90E−01	2.572E−01
27.2	5.51E−02	1.82E−01	2.01E−01	4.38E−01	2.110E−01
27.4	5.44E−02	1.82E−01	1.96E−01	4.33E−01	2.064E−01
31.0	4.45E−02	1.83E−01	1.31E−01	3.58E−01	1.429E−01
31.7	4.28E−02	1.83E−01	1.22E−01	3.48E−01	1.340E−01
35.5	3.53E−02	1.83E−01	8.40E−02	3.03E−01	9.803E−02
			(b)		
22.1	6.79E−02	1.76E−01	3.92E−01	6.36E−01	4.000E−01
24.9	5.63E−02	1.78E−01	2.68E−01	5.02E−01	2.772E−01
25.5	5.42E−02	1.78E−01	2.48E−01	4.80E−01	2.575E−01
27.2	4.88E−02	1.79E−01	2.02E−01	4.29E−01	2.122E−01
27.4	4.83E−02	1.79E−01	1.97E−01	4.24E−01	2.073E−01
31.0	3.94E−02	1.79E−01	1.33E−01	3.51E−01	1.447E−01
31.7	3.79E−02	1.79E−01	1.23E−01	3.41E−01	1.350E−01
35.5	3.13E−02	1.79E−01	8.56E−02	2.96E−01	9.928E−02

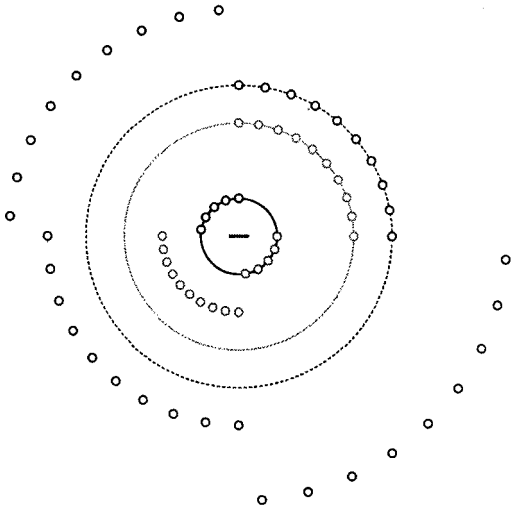

FIG. 3. Plastic water phantom used for measuring the angular dependence of the dose rate from the I-Plant Model 3500 seed. The seed in the center is perpendicular to the LiF TLD rods.

thin spherical shell of water in an otherwise homogeneous plastic water medium.

E. Dose rate constant

The dose rate constant, Λ, was measured with TLD rods in a solid water phantom for both the I-Plant Model 3500 seed and the Model 6711 seed. The measured dose rate per unit air kerma strength was calculated from

$$\dot{D}(r,\theta)=\frac{D_{\mathrm{Co}}C_E C_{\mathrm{med}}(r)R(r,\theta)}{S_{k,0}[1-\exp(-\lambda t)]}, \tag{7}$$

where D_{Co} is the ^{60}Co dose corresponding to the TLD reading $R(r,\theta)$, $S_{k,0}$ is the initial air kerma strength, λ is the decay constant of ^{125}I, C_E is the ratio of the response to ^{125}I photons to the response to ^{60}Co gamma rays, and $C_{\mathrm{med}}(r)$ is a distance-dependent correction for replacing water by the phantom medium. C_E was found by Weaver to be $1.39+0.03$.[39] $C_{\mathrm{med}}(r)$ was found by simulating a point source in water and in the phantom medium by Luxton[29] to be 1.038 at $r=1$ cm for solid water. The air kerma strength of the I-Plant Model 3500 seed was measured (in June 2000) by NIST, while that of the Model 6711 seed was measured (also in June 2000) by an AAPM Accredited Dosimetry Laboratory (K&S Associates, Nashville, TN). Both air kerma strength measurements were based on the revised NIST standard of 1 January 1999.[14,40] The dose rate constant for the I-Plant Model 3500 seed was determined from

$$\Lambda_{3500}=\left[\frac{\dot{D}_{3500}(1\ \mathrm{cm},\pi/2)/S_{k,3500}}{\dot{D}_{6711}(1\ \mathrm{cm},\pi/2)/S_{k,6711}}\right]\Lambda_{6711}. \tag{8}$$

Three separate measurements of the dose rate, each with six TLD rods, were made for each seed.

TABLE V. Radial dose function for the I-Plant Model 3500 ^{125}I seed.

r(cm)	Measured in plastic $g(r)$	Plastic to water correction	Corrected water $g(r)$	Exponential sum fit to water $g(r)$
0.5	1.023	0.989	1.012	1.026
1.0	1.000	1.000	1.000	1.000
1.5	0.959	1.004	0.962	0.936
2.0	0.856	1.014	0.868	0.855
2.5	0.752	1.018	0.765	0.770
3.0	0.648	1.027	0.666	0.687
3.5	0.570	1.030	0.587	0.609
4.0	0.524	1.038	0.544	0.537
4.5	0.455	1.045	0.476	0.473
5.0	0.404	1.049	0.424	0.416
6.0	0.307	1.057	0.324	0.320
7.0	0.232	1.071	0.248	0.246

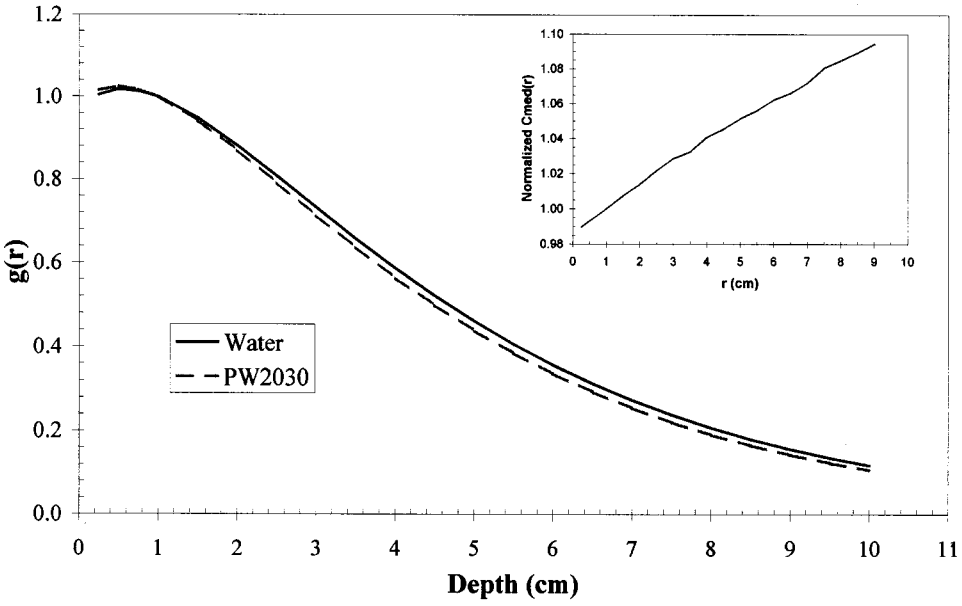

FIG. 4. Radial dose functions $g(r)$ calculated from MCNP4B Monte Carlo simulations for water and PW2030 water-equivalent plastic. In the inset is the plastic-to-water correction factor used to convert the radial dose function measured in PW2030 to the radial dose function in water.

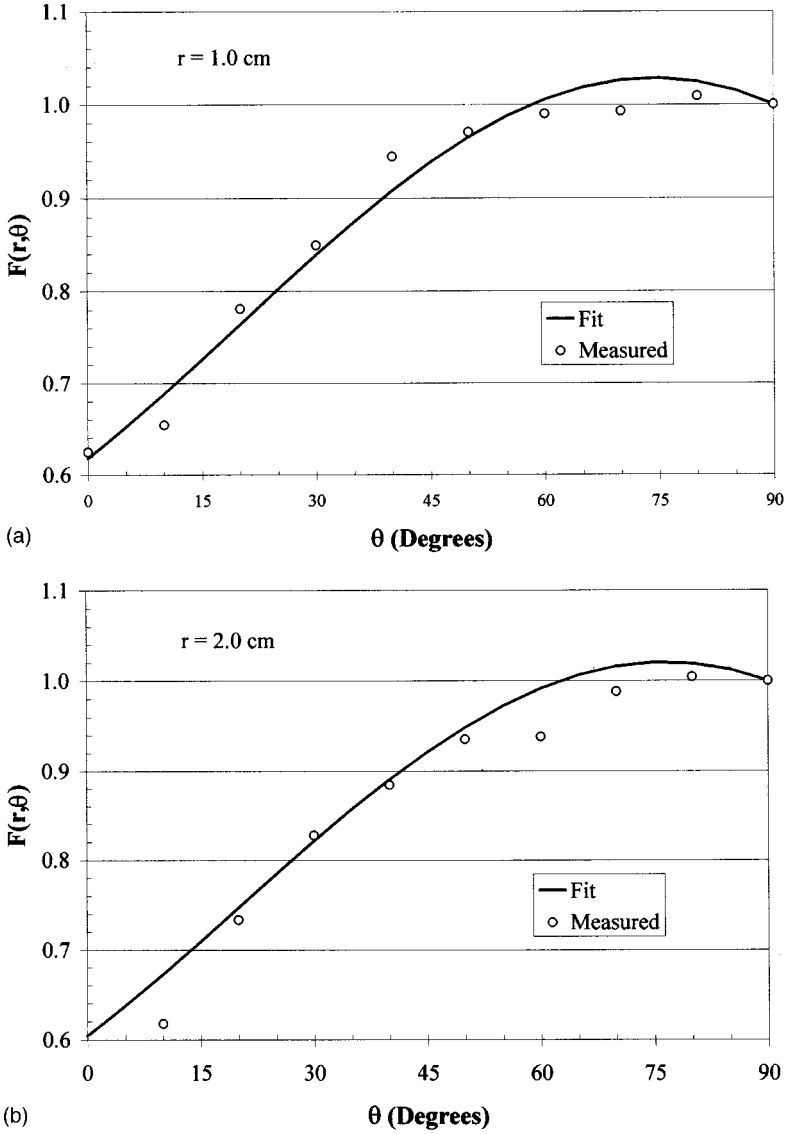

FIG. 5. Anisotropy function, $F(r,\theta)$, calculated from data measured with phantom in Fig. 3, and fit. The radii are 1, 2, 3, 4, 5, 7 cm in (A)–(F), respectively.

F. Radial dependence

The radial dose function was measured with TLD rods in the plastic water phantoms shown in Fig. 2. The dose rates were calculated according to Eq. (7) above and normalized to the dose rate at 1 cm. At each radial distance, the standard deviation of all the measurements was less than 4% of the average, and most were less than 3%. The required values of $C_{\text{med}}(r)$ for plastic water were calculated in the manner described above, except that the MCNP4B code was used.[29] In particular, MCNP ''$*f8$'' tallies were used; these sum the net energy deposited in each tally cell from each interaction in that cell. All of the tally cells were spherical shells whose thickness was chosen according to the criterion of Luxton and Joszef[41]

$$1\% \geqslant (R_\nu/R_m)^2 - 1,$$

where

$$R_m = (R_i + R_o)/2$$

is the mean of the inner and outer radii of the shell, R_i and R_o, and

$$R_\nu = [(R_i^3 + R_o^3)/2]^{1/3}$$

is the radius of a sphere whose volume is the average of the volumes enclosed by the inner and outer spherical surfaces. The photon and electron energy cutoffs were set at 1 keV and 20 keV, respectively, just as they were by Luxton.[29] $C_{\text{med}}(r)$ and $g(r)$ were calculated for homogeneous media consisting of water and PW2030. The simulations were benchmarked by repeating them for the WT-1 Solid Water and polymethylmethacrylate (PMMA) compositions and the Model 6711 spectrum given in Luxton's paper.[29] The results agreed with Luxton's to within 1% for distances of 2 cm or less and 2% for distances up to 10 cm. For each of the plastics, simulations were performed for two cases: a homogeneous medium and a single spherical shell of water (the tally cell) in an otherwise homogeneous medium. In agreement with Luxton, the authors found that, for a given plastic,

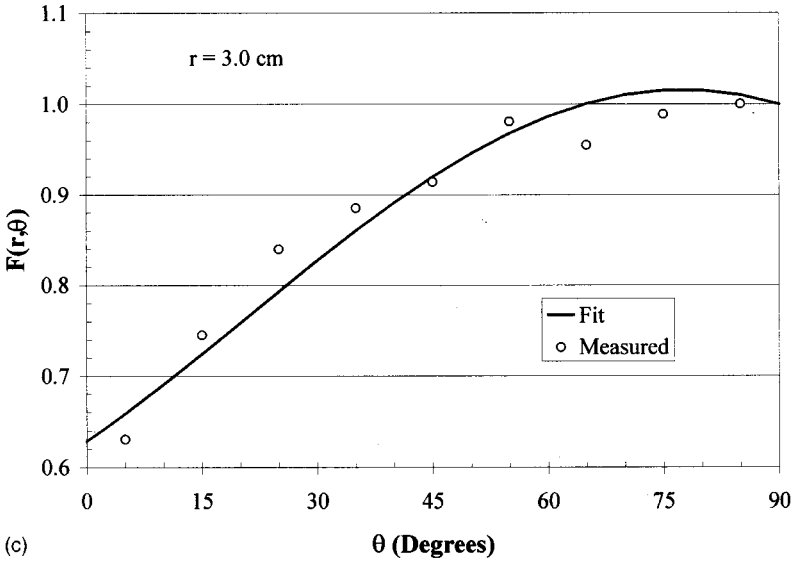

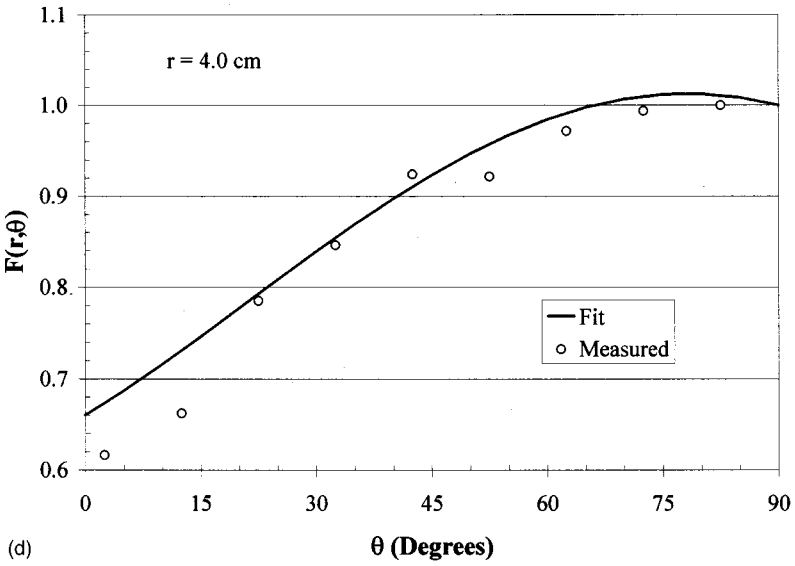

FIG. 5 (*Continued.*)

the $g(r)$ function calculated from the results is the same, to within the estimated error in the tallies, in both cases. The $g(r)$ function for water and plastic water are shown in Fig. 4.

After normalizing at $r=1$ cm, $C_{\text{med}}(r)$ varies from 0.99 at 0.5 cm to 1.07 at 7 cm as shown in Table V (Plastic to Water Correction) and the inset in Fig. 4. When the simulations were repeated with the density of the PW2030 set to 1.000 g/cm^3, the normalized $C_{\text{med}}(r)$ varied only from 0.99 at 0.5 cm to 1.03 at 7 cm. This shows that the difference in density between PW2030 and water is more important than the difference in composition in this photon energy range.

G. Angular dependence

The dependence of the dose rate on zenith angle (normalized to 90 deg) was measured with TLD rods in the phantom shown in Fig. 3. Three separate determinations of the curves at radial distances of 1, 2, and 3 cm were made, and the results were averaged. For each point on those curves, the standard deviation of all the measurements was less than 6% of the average, and for most it was less than 3%. The curves at 1.5, 2.5, 3.5, 4, 5, 6, and 7 cm were determined only once.

III. RESULTS

A. Dose rate constant

The dose rate constant was found, by direct comparison of calibrated I-Plant Model 3500 and Model 6711 seeds in a solid water phantom, to be 1.01 (cGy/h)/U. The value of the dose rate constant for the Model 6711 seed was taken from the literature[40] to be 0.98 (cGy/h)/U.

B. Radial dose function

The dose rates calculated according to Eq. (7) from the TLD rods exposed in the phantoms in Fig. 2 were used in Eq. (3) to calculate the radial dose function in plastic water, $g(r)$. The radial dose function was then corrected using the ratio of dose-to-water to dose to dose to water in plastic

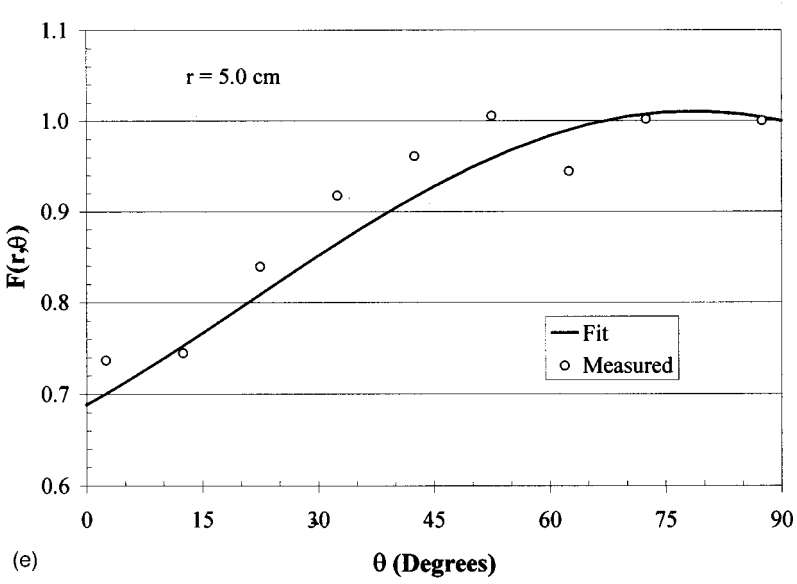

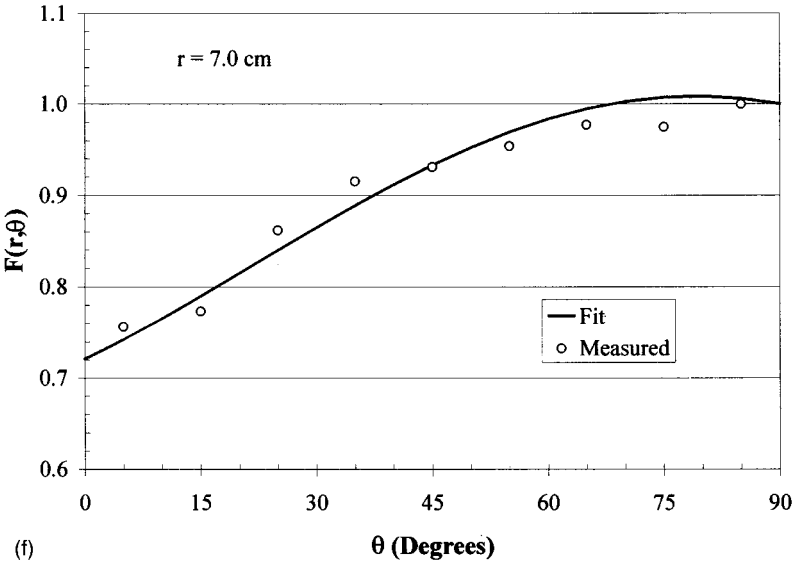

FIG. 5 (*Continued.*)

water, to obtain the radial dose function in water. The radial dose function in water was fit, using the Levenberg–Marquardt method and commercially available software (Mathematica 4.0, Wolfram Research, Champaign, IL), with the expression of Furhang and Anderson[42]

$$g(r)=C_1e^{-\mu_1 r}+C_2e^{-\mu_2 r}, \tag{9}$$

where: $C_1=1.5807$, $\mu_1=0.2655$, $C_2=-0.6032$, $\mu_2=1.0445$. The $g(r)$ values calculated from the data and the fit in Eq. (9) are given in Table V. A polynomial fit may be used for distances from 0 to 7 cm only; this fit has the form

$$g(r)=a_0+a_1r+a_2r^2+a_3r^3+a_4r^4+a_5r^5, \tag{10}$$

where: $a_0=0.977\,612$, $a_1=0.169\,935$, $a_2=-0.188\,298$, $a_3=4.521\,07\times10^{-2}$, $a_4=-4.633\,78\times10^{-3}$, and $a_5=1.739\,50\times10^{-4}$. Both fits to the radial dose function are compared to the values calculated from the data (see in Fig. 6).

C. Anisotropy function

Values of the anisotropy function, $F(r,\theta)$, were calculated from the measured dose rate versus zenith angle curve according to Eq. (4). The values were fit by a family of curves suggested by Furhang and Anderson[42]

$$F(r,\theta)=1-a+b\,\theta\cos(\theta)e^{cr}, \tag{11}$$

where $a=a_0+a_1r$, $b=b_0+b_1r$, and $c=c_0+c_1r$.

With θ in rads and r in cm, the best fit parameters were found by the Levenberg–Marquardt method (Mathematica 4.0, Wolfram Research) to be $a_0=0.250\,546$, $a_1=0.360\,028$, $b_0=-0.315\,912$, $b_1=-0.288\,315$, $c_0=-0.499\,94$, and $c_1=0.024\,544\,8$. The fitted values are presented in Table VI and plotted in Figs. 5(a)–5(f).

The anisotropy factor, $\phi_{an}(r)$, was calculated from the values in Table VI by averaging over all solid angles as described in the TG-43 report. The anisotropy factor, also given in Table VI was found to be between 0.94 and 0.96 at

TABLE VI. Anisotropy function for the I-Plant Model 3500 ^{125}I seed from fit to data.

r (cm)	1.0	1.5	2.0	2.5	3.0	3.5	4.0	5.0	6.0	7.0
$\phi_{an}(r)$	0.956	0.948	0.944	0.943	0.943	0.944	0.945	0.948	0.951	0.952
r (cm) θ	1.0	1.5	2.0	2.5	3.0	3.5	4.0	5.0	6.0	7.0
0.0	0.618	0.603	0.604	0.614	0.629	0.644	0.660	0.688	0.709	0.721
2.5	0.635	0.620	0.621	0.630	0.643	0.658	0.673	0.700	0.720	0.732
5.0	0.652	0.637	0.637	0.646	0.659	0.673	0.687	0.713	0.732	0.743
10.0	0.688	0.674	0.673	0.680	0.691	0.703	0.716	0.739	0.756	0.766
15.0	0.726	0.711	0.710	0.715	0.724	0.735	0.746	0.766	0.781	0.790
20.0	0.764	0.750	0.747	0.751	0.759	0.768	0.777	0.795	0.807	0.815
25.0	0.802	0.788	0.785	0.787	0.793	0.801	0.809	0.823	0.834	0.840
30.0	0.839	0.826	0.822	0.823	0.827	0.833	0.839	0.851	0.860	0.865
35.0	0.875	0.862	0.857	0.857	0.860	0.864	0.869	0.878	0.885	0.889
40.0	0.908	0.896	0.891	0.890	0.891	0.894	0.897	0.904	0.909	0.912
45.0	0.938	0.927	0.921	0.920	0.920	0.921	0.923	0.928	0.931	0.933
50.0	0.965	0.955	0.949	0.946	0.946	0.946	0.947	0.949	0.951	0.952
55.0	0.988	0.978	0.973	0.969	0.968	0.967	0.967	0.968	0.969	0.969
60.0	1.006	0.997	0.992	0.988	0.986	0.985	0.984	0.984	0.984	0.983
65.0	1.019	1.011	1.007	1.003	1.001	0.999	0.998	0.996	0.995	0.995
70.0	1.026	1.020	1.016	1.013	1.010	1.008	1.007	1.005	1.003	1.003
75.0	1.028	1.024	1.020	1.018	1.015	1.013	1.012	1.010	1.008	1.007
80.0	1.025	1.022	1.019	1.017	1.015	1.014	1.012	1.011	1.009	1.008
85.0	1.015	1.014	1.012	1.011	1.010	1.009	1.008	1.007	1.007	1.006
90.0	1.000	1.000	1.000	1.000	1.000	1.000	1.000	1.000	1.000	1.000

all radii. The average anisotropy factor, $\overline{\phi}_{an}$, was also found by averaging over all values of r from 1 to 7 cm to be 0.95.

IV. DISCUSSION AND CONCLUSIONS

Since the design of the new I-Plant Model 3500 seed resembles those of two other ^{125}I seeds, the Model 6711 (Medi-Physics, Inc., Arlington Heights, IL) and the Symmetra (Bebig GmbH, Berlin, Germany), it is worthwhile comparing its dose distribution to theirs. The measured dose rate constant, 1.01 cGy/U, is slightly higher than the accepted value[40] for the Model 6711, 0.98 cGy/U, and approximately the same as that of the Symmetra, 1.00–1.01 cGy/U.[21] The radial dose function falls off more slowly than that of the Model 6711, which can be expected since the photon spectrum is harder.[43] Indeed, the monoenergetic point dose kernels, determined by Luxton and Joszef using the EGS4 Monte Carlo code,[41] were averaged over the measured I-Plant spectrum in Table I and, as shown in Fig. 6, the radial dose

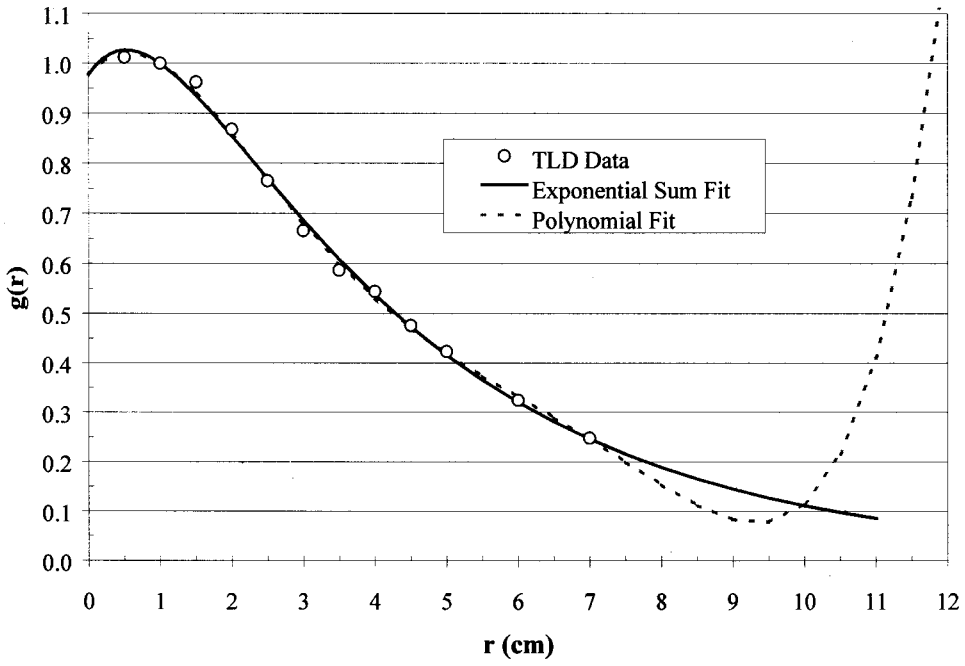

FIG. 6. Radial dose function, $g(r)$, in water of I-Plant Model 3500 seed measured with TLD rods in the phantoms in Fig. 2. Also shown are fits to the data using the exponential sum expression in Eq. (9) and a fifth-order polynomial.

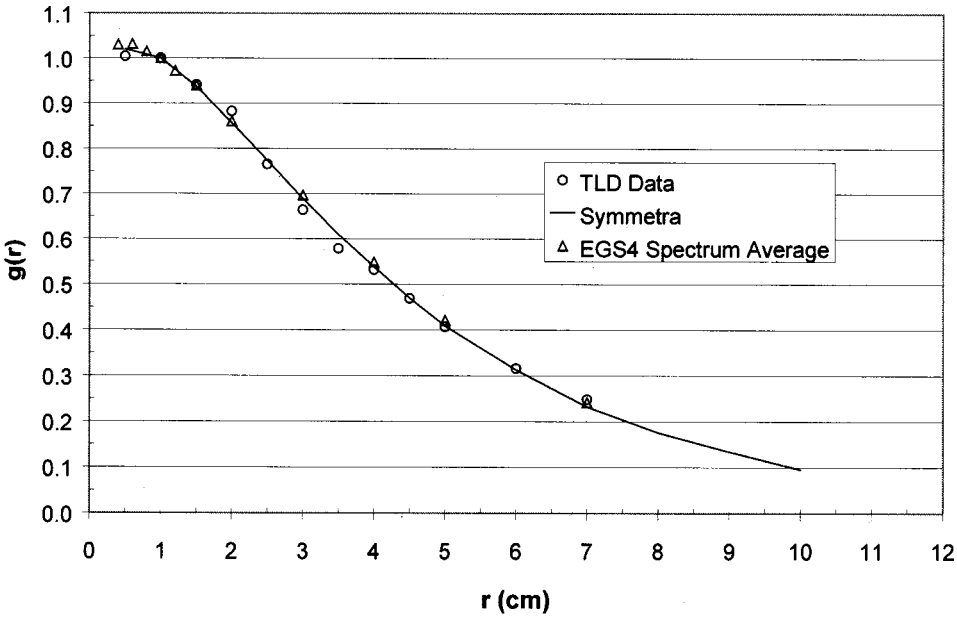

FIG. 7. Comparison of measured radial dose function, $g(r)$, in water of the I-Plant Model 3500 seed to that predicted for the Symmetra seed by Hedtjarn *et al.* and an average over the measured I-Plant seed spectrum of the monoenergetic point dose distributions calculated by Luxton and Joszef.

function for such a point source is practically the same as that calculated from the data. Since the I-Plant design is even more similar to that of the Symmetra, it is not surprising that the radial dose function is almost the same, as shown in Fig. 7. The angular dependence of the dose rate is more like that of the Symmetra[21] than that of the 6711.[23,28,30]

The authors have used a brachytherapy treatment planning system (Pinnacle3, ADAC Labs, Milpitas, CA), which employs a point source approximation, to calculate dose distributions from the Model 6711 seed and the new I-Plant seed. The differences were seen to be small. For example for two sample implants, each including 27 seeds arranged in a 2 cm by 2 cm grid with 1 cm spacing, the distances from the center of the implant to the isodose lines were the same to within 2 mm, for distances up to 3 cm.

In conclusion, the I-Plant seed, although made by a novel process, produces a dose distribution that is similar to those from other seeds. This should greatly facilitate its use in interstitial brachytherapy.

[1] C. Stannard, R. Sealy, D. Shackleton, J. Hill, and J. Korrubel, ''The use of iodine-125 plaques in the treatment of retinoblastoma,'' Ophthalmic Paediatr. Genet. **8**, 89–93 (1987).
[2] H. Schilling, N. Bornfeld, W. Friedrichs, D. Pauleikhoff, W. Sauerwein, and A. Wessing, ''Histopathologic findings in large uveal melanomas after brachytherapy with iodine 125 ophthalmic plaques,'' Ger. J. Ophthalmol. **3**, 232–238 (1994).
[3] D. H. Abramson, D. Fass, B. McCormick, C. A. Servodidio, J. D. Piro, and L. L. Anderson, ''Implant brachytherapy: a novel treatment for recurrent orbital rhabdomyosarcoma,'' J. Aapos. **1**, 154–157 (1997).
[4] S. K. Ray, R. Bhatnagar, W. F. Hartsell, and G. R. Desai, ''Review of eye plaque dosimetry based on AAPM Task Group 43 recommendations. American Association of Physicists in Medicine,'' Int. J. Radiat. Oncol., Biol., Phys. **41**, 701–706 (1998).
[5] P. T. Finger, A. Berson, and A. Szechter, ''Palladium-103 plaque radiotherapy for choroidal melanoma: Results of a 7-year study,'' Ophthalmology (Philadelphia) **106**, 606–613 (1999).
[6] P. H. Gutin, T. L. Phillips, W. M. Wara, S. A. Leibel, Y. Hosobuchi, V. A. Levin, K. A. Weaver, and S. Lamb, ''Brachytherapy of recurrent malignant brain tumors with removable high-activity iodine-125 sources,'' J. Neurosurg. **60**, 61–68 (1984).
[7] A. Etou, F. Mundinger, M. Mohadjer, and W. Birg, ''Stereotactic interstitial irradiation of diencephalic tumors with iridium 192 and iodine 125: 10 years follow-up and comparison with other treatments,'' Childs Nerv. Syst. **5**, 140–143 (1989).
[8] E. A. Healey, R. C. Shamberger, H. E. Grier, J. S. Loeffler, and N. J. Tarbell, ''A 10-year experience of pediatric brachytherapy,'' Int. J. Radiat. Oncol., Biol., Phys. **32**, 451–455 (1995).
[9] M. W. McDermott, P. K. Sneed, and P. H. Gutin, ''Interstitial brachytherapy for malignant brain tumors,'' Semin. Surg. Oncol. **14**, 79–87 (1998).
[10] M. R. Storey, R. C. Landgren, J. L. Cottone, J. W. Stallings, C. W. Logan, L. P. Fraiser, C. S. Ross, R. J. Kock, L. W. Berkley, and M. Hauer-Jensen, ''Transperineal 125iodine implantation for treatment of clinically localized prostate cancer: 5-year tumor control and morbidity,'' Int. J. Radiat. Oncol., Biol., Phys. **43**, 565–570 (1999).
[11] S. Nag, D. Beyer, J. Friedland, P. Grimm, and R. Nath, ''American Brachytherapy Society (ABS) recommendations for transperineal permanent brachytherapy of prostate cancer,'' Int. J. Radiat. Oncol., Biol., Phys. **44**, 789–799 (1999).
[12] C. J. Mettlin, G. P. Murphy, C. J. McDonald, and H. R. Menck, ''The National Cancer Data base Report on increased use of brachytherapy for the treatment of patients with prostate carcinoma in the U.S.,'' Cancer (N.Y.) **86**, 1877–1882 (1999).
[13] B. O. Jose, J. L. Bailen, F. H. Albrink, G. S. Steinbock, M. S. Cornett, D. C. Benson, W. K. Schmied, R. N. Medley, W. J. Spanos, K. J. Paris, P. D. Koerner, R. A. Gatenby, D. L. Wilson, and R. Meyer, ''Brachytherapy in early prostate cancer—early experience,'' J. Ky. Med. Assoc. **97**, 12–26 (1999).
[14] Y. Yu, L. L. Anderson, Z. Li, D. E. Mellenberg, R. Nath, M. C. Schell, F. M. Waterman, A. Wu, and J. C. Blasko, ''Permanent prostate seed implant brachytherapy: Report of the American Association of Physicists in Medicine Task Group No. 64,'' Med. Phys. **26**, 2054–2076 (1999).
[15] J. P. Ciezki, E. A. Klein, K. W. Angermeier, J. Ulchaker, C. D. Zippe, and D. A. Wilkinson, ''Cost comparison of radical prostatectomy and transperineal brachytherapy for localized prostate cancer,'' Urology **55**, 68–72 (2000).
[16] R. M. Benoit, M. J. Naslund, and J. K. Cohen, ''Complications after prostate brachytherapy in the Medicare population,'' Urology **55**, 91–96 (2000).
[17] J. G. Wierzbicki, M. J. Rivard, D. S. Waid, and V. E. Arterbery, ''Calculated dosimetric parameters of the IoGold 125I source model 3631-A,'' Med. Phys. **25**, 2197–2199 (1998).
[18] R. E. Wallace and J. J. Fan, ''Evaluation of a new brachytherapy iodine-125 source by AAPM TG43 formalism,'' Med. Phys. **25**, 2190–2196 (1998).
[19] R. E. Wallace and J. J. Fan, ''Report on the dosimetry of a new design

125Iodine brachytherapy source,'' Med. Phys. **26**, 1925–1931 (1999).
[20] Z. Li, J. J. Fan, and J. R. Palta, ''Experimental measurements of dosimetric parameters on the transverse axis of a new 125I source,'' Med. Phys. **27**, 1275–1280 (2000).
[21] H. Hedtjarn, G. A. Carlsson, and J. F. Williamson, ''Monte Carlo-aided dosimetry of the Symmetra model I25.S06 125I, interstitial brachytherapy seed,'' Med. Phys. **27**, 1076–1085 (2000).
[22] A. S. Meigooni, D. M. Gearheart, and K. Sowards, ''Experimental determination of dosimetric characteristics of Best ^{125}I brachytherapy source,'' Med. Phys. **27**, 2168–2173 (2000).
[23] C. C. Ling, M. C. Schell, E. D. Yorke, B. B. Palos, and D. O. Kubiatowicz, ''Two-dimensional dose distribution of 125I seeds,'' Med. Phys. **12**, 652–655 (1985).
[24] G. S. Burns and D. E. Raeside, ''Two-dimensional dose distribution around a commercial 125I seed,'' Med. Phys. **15**, 56–60 (1988).
[25] K. A. Weaver, V. Smith, D. Huang, C. Barnett, M. C. Schell, and C. Ling, ''Dose parameters of 125I and 192Ir seed sources,'' Med. Phys. **16**, 636–643 (1989).
[26] R. Nath, A. S. Meigooni, and J. A. Meli, ''Dosimetry on transverse axes of 125I and 192Ir interstitial brachytherapy sources,'' Med. Phys. **17**, 1032–1040 (1990).
[27] A. S. Meigooni and R. Nath, ''A comparison of radial dose functions for 103Pd, 125I, 145Sm, 241Am, 169Yb, 192Ir, and 137Cs brachytherapy sources,'' Int. J. Radiat. Oncol., Biol., Phys. **22**, 1125–1130 (1992).
[28] R. Nath, A. S. Meigooni, P. Muench, and A. Melillo, ''Anisotropy functions for 103Pd, 125I, and 192Ir interstitial brachytherapy sources,'' Med. Phys. **20**, 1465–1473 (1993).
[29] G. Luxton, ''Comparison of radiation dosimetry in water and in solid phantom materials for I-125 and Pd-103 brachytherapy sources: EGS4 Monte Carlo study,'' Med. Phys. **21**, 631–641 (1994).
[30] K. Weaver, ''Anisotropy functions for 125I and 103Pd sources,'' Med. Phys. **25**, 2271–2278 (1998).
[31] R. Nath, L. L. Anderson, G. Luxton, K. A. Weaver, J. F. Williamson, and A. S. Meigooni, ''Dosimetry of interstitial brachytherapy sources: Recommendations of the AAPM Radiation Therapy Committee Task Group No. 43. American Association of Physicists in Medicine,'' Med. Phys. **22**, 209–234 (1995).
[32] J. Williamson, B. M. Coursey, L. A. DeWerd, W. F. Hanson, and R. Nath, ''Dosimetric prerequisites for routine clinical use of new low energy photon interstitial brachytherapy sources. Recommendations of the American Association of Physicists in Medicine Radiation Therapy Committee. Ad Hoc Subcommittee of the Radiation Therapy Committee,'' Med. Phys. **25**, 2269–2270 (1998).
[33] J. F. Williamson, ''Comparison of measured and calculated dose rates in water near I-125 and Ir-192 seeds,'' Med. Phys. **18**, 776–786 (1991).
[34] R. Nath and A. Melillo, ''Characteristics of 125I source for interstitial brachytherapy,'' Med. Phys. **20**, 1475–1483 (1993).
[35] AAPM ''A protocol for the determination of absorbed dose from high-energy photon and electron beams,'' Med. Phys. **10**, 741–771 (1983).
[36] J. F. Briesmeister, Report No. LA-12625-M, 1997.
[37] J. J. DeMarco, J. B. Smathers, C. M. Burnison, Q. K. Ncube, and T. D. Solberg, ''CT-based dosimetry calculations for 125I prostate implants,'' Int. J. Radiat. Oncol., Biol., Phys. **45**, 1347–1353 (1999).
[38] J. S. Hendricks and J. D. Court, Report No. LA-13181, 1996.
[39] K. A. Weaver, ''Response of LiF powder to ^{125}I photons,'' Med. Phys. **11**, 850–854 (1984).
[40] J. F. Williamson, B. M. Coursey, L. A. DeWerd, W. F. Hanson, R. Nath, and G. Ibbott, ''Guidance to users of Nycomed Amersham and North American Scientific, Inc., I-125 interstitial sources: Dosimetry and calibration changes: Recommendations of the American Association of Physicists in Medicine Radiation Therapy Committee Ad Hoc Subcommittee on Low-Energy Seed Dosimetry,'' Med. Phys. **26**, 570–573 (1999).
[41] G. Luxton and G. Jozsef, ''Radial dose distribution, dose to water and dose rate constant for monoenergetic photon point sources from 10 keV to 2 MeV:EGS4 Monte Carlo model calculation,'' Med. Phys. **26**, 2531–2538 (1999).
[42] E. E. Furhang and L. L. Anderson, ''Functional fitting of interstitial brachytherapy dosimetry data recommended by the AAPM Radiation Therapy Committee Task Group 43. American Association of Physicists in Medicine,'' Med. Phys. **26**, 153–160 (1999).
[43] C. C. Ling, E. D. Yorke, L. J. Spiro, D. Kubiatowicz, and D. Bennett, ''Physical dosimetry of ^{125}I seeds of a new design for interstitial implant,'' Int. J. Radiat. Oncol., Biol., Phys. **9**, 1747–1752 (1983).